

EXPERIMENTAL INVESTIGATION OF A SPATIOTEMPORAL STRUCTURE OF A SPHERICAL WAVE REFLECTED FROM A PLANE MIRROR

A.P. Ivanov, G.Ya. Patrushev, and A.P. Rostov

*Institute of Atmospheric Optics,
Siberian Branch of the Russian Academy of Sciences, Tomsk
Received February 29, 1992*

Some results of experimental investigation of a spatiotemporal structure of a spherical wave reflected from a plane mirror in the turbulent atmosphere are presented. A low-frequency shift in temporal spectra of strong intensity fluctuations depending on the relation between the fluctuational and average components of wind velocity in the direction perpendicular to the propagation path is found as the observation point is removed from the strictly backward direction. An inhomogeneity in spatial correlation of strong intensity fluctuations in the receiver plane is determined. Cross correlation functions for various ratios of fluctuational component to the average value of wind velocity in the direction perpendicular to the propagation path are analyzed.

The spatiotemporal structure of optical waves during their propagation on straight paths through a turbulent atmospheric layer was widely investigated both theoretically and experimentally. Detailed review of these investigations was given in Ref. 1. Propagation of radiation on paths with reflection is characterized by a number of specific effects due to the double passage of the same inhomogeneities in the forward and backward directions. In some situations an increase in the average intensity of reflected radiation near the strictly backward direction,^{1,2,3} intensification of intensity fluctuations,² and transformation of the spatiotemporal structure^{1,2,4} are observed.

In this paper the experimental investigation of spatiotemporal structure of a spherical wave reflected from a plane specular surface in the turbulent atmosphere is described. The experiment was performed on real atmospheric paths of lengths $L = 400$ and 800 m located above an even underlying surface. The setup and measurement technique were described in detail in Ref. 3. The signals of reflected radiation were detected near the optical axis in the plane perpendicular to the propagation direction. The electric signals from the photodetectors were stored on a code disk unit (CDU) using an ADC (see Ref. 5) which allowed us to record up to eight analog signals with a maximum sampling rate of 20 kHz and a dynamic range of 72 dB (12-bit ADC). Recorded realizations were processed in real time with subsequent calculation of the average value and variance in each channel during measurements. A complete statistical analysis was made on a stationary complex in the laboratory.

Pressure, humidity, and temperature along the path as well as the average (V_{\perp}) and fluctuational (σ_{\perp}) components of wind velocity in the direction perpendicular to the propagation path were measured, synchronously with recording on the CDU, with the help of an acoustic anemometer⁸ placed 100 m apart from the measurement pavilion. An additional path was arranged parallel to the main propagation path to determine the structure constant of the refractive index C_n^2 and to calculate subsequently the parameter $\beta_0 = [1.23 C_n^2 \kappa^{7/6} (2L)^{11/6}]^{1/2}$, which describes the turbulence intensity on the path of length $2L$, where $\kappa = 2\pi\lambda$ is the wave number.

The temporal spectra of the intensity fluctuations were calculated by the fast Fourier transform method. The spectra were smoothed over segments of realizations and over neighboring frequencies so that the number of degrees of freedom was no less than 700, which yielded about 4% variance of the spectrum estimates over the entire spectral range.⁶

The results of experimental estimates of the temporal spectra of the intensity fluctuations are shown in Fig. 1 for two limiting values of the ratio σ_{\perp}/V_{\perp} obtained in these measurements.

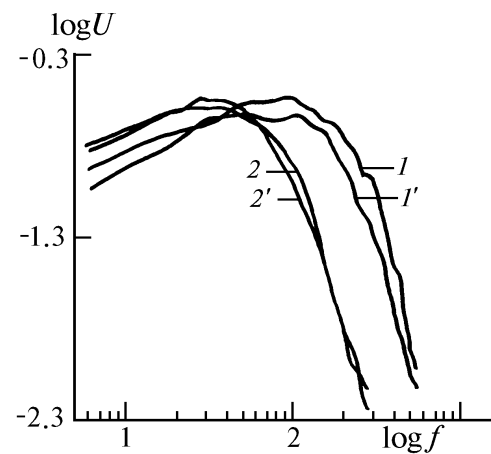


FIG. 1 The normalized spectrum $U(f)$ of strong intensity fluctuations for a spherical wave reflected from a mirror as a function of frequency f . $\sigma_{\perp}/V_{\perp} \approx 0.3$ (1 and 1') and 4 (2 and 2').

The logarithm of the frequency f (Hz) is plotted on the abscissa and the logarithm of the dimensionless spectrum $U = W(f) f / \sigma_I^2$ is plotted on the ordinate ($W(f)$ is the frequency spectrum and σ_I is the variance of the intensity fluctuations). The given estimates were obtained for strong fluctuations of the intensity along the path for $\beta_0 \approx 3.8-4.2$. An analysis of the data shows that

the spectra of the intensity fluctuations differ for different points of observation in the receiver plane. As can be seen from Fig. 1, the spectrum is shifted toward the low-frequency region (curve 1, $\rho = 0.1\sqrt{2\lambda L}$) when the point of observation is removed from the source optical axis (curve 1', $\rho = 0.7\sqrt{2\lambda L}$) which in this case coincides with the strictly backward direction. In Ref. 4 the shift of the spectra for weak fluctuations of the intensity was pointed out, and physical interpretation of the observed effect was given. The dependence of the shift from the ratio σ_{\perp}/V_{\perp} should be noted. Curves 2 and 2' were obtained for the same position of the receivers and the same values of β_0 . However, one can see that increasing the fluctuation component σ_{\perp} of the wind velocity in the direction perpendicular to the propagation path in comparison with its average value V_{\perp} leads to smearing of the spectrum shift and for $\sigma_{\perp}/V_{\perp} \approx 4$ (curves 2 and 2') the difference between the spectra is within the limits of the statistical error of measurements. Different position of the spectra 1, 1' and 2, 2' on the frequency axis is explained by different values of σ_{\perp} and V_{\perp} during the measurement period. Introduction of the dimensionless frequency $\Omega = f/f_{0\text{ef}} = f/(\sqrt{\sigma_{\perp}^2 + V_{\perp}^2}/\sqrt{2\pi\lambda 2L})$ by analogy with Ref. 7 leads to the fact that the estimates of temporal spectra of fluctuations of the reflected wave intensity come closer (see Fig. 2). In this case the low-frequency shift of the spectrum 1' relative to the spectrum 1 remained the same on this scale.

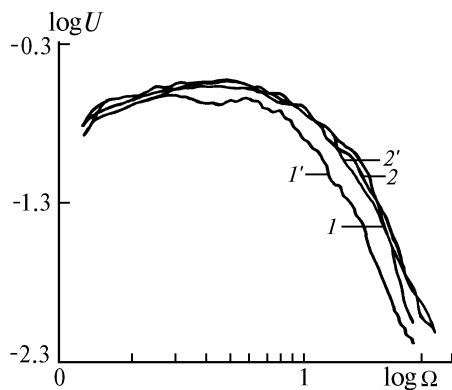


FIG. 2 The normalized spectrum $U(\Omega)$ of strong intensity fluctuations for a spherical wave reflected from a mirror as a function of the dimensionless frequency Ω . $\sigma_{\perp}/V_{\perp} \approx 0.3$ (1 and 1') and 4 (2 and 2').

The results of experimental study of the spatial correlation structure for strong intensity fluctuations of a spherical wave reflected from a mirror are shown in Fig. 3 (curves 1 and 2) for $\beta_0 \approx 4.6$. Behavior of the correlation coefficient $b_{I,R}(\mathbf{R}, \rho)$ depends on the position of the observation points ρ_1 and ρ_2 about the optical axis of the source, where $\mathbf{R} = (\rho_1 + \rho_2)/2$, $\rho = \rho_1 - \rho_2$, and $\rho = |\rho|$. Curve 1 corresponds to the asymmetrical position of the observation points about the optical axis of the source $\mathbf{R} = \rho/2$, and curve 2 corresponds to the symmetrical position $\mathbf{R} = 0$. The standard deviation of experimental estimate of the correlation coefficient calculated by the technique described in Ref. 6 was in the range 5–10% depending on the value of the correlation coefficient. For

comparison, the figure shows the results of numerical calculation of $b_{I,R}(\mathbf{R}, \rho)$ (curves 1' and 2') by the formulas taken from Refs. 1 and 2. In the case of axisymmetrical position of the receivers at $\mathbf{R} = 0$, the calculational formula had the form

$$b_{I,R}(\mathbf{R}, \rho) = [\alpha(\rho/2)]^{-1} [\exp\{-4(\rho/\rho_c)^{5/3}\} + \exp\{-2(\rho/2\rho_c)^{5/3}\} + 2\exp\{-2(\rho/\rho_c)^{5/3}\} + \exp\{-16/3(\rho/2\rho_c)^{5/3}\}],$$

while for their asymmetrical position when one of the receivers was placed near the optical axis of the source, at $\mathbf{R} = \rho/2$, the formula was

$$b_{I,R}(\mathbf{R}, \rho) = [2\sqrt{a(r)}]^{-1} [3\exp\{-4(r/r_c)^{5/3}\} + \exp\{-2(\rho/\rho_c)^{5/3}\}],$$

where $\alpha(\rho) = 1 + \exp\{-4(\rho/\rho_c)^{5/3}\} + 2\exp\{-2(\rho/\rho_c)^{5/3}\}$. The coherence radius ρ_c under experimental conditions was calculated by the formula $\rho_c = 1.6(1.45 C_n^2 k^2 L)^{-3/5}$ (see Refs. 1 and 2).

As one can see from Fig. 3, in the case of axisymmetrical ($\mathbf{R} = 0$) separation of the receivers the degree of correlation for strong fluctuations of the intensity of a spherical wave reflected from a mirror is higher for both experimental (curve 2) and calculated (curve 2') data. However, the experimental value of the correlation coefficient is much greater than the calculated values for separation $\rho/\rho_c \gg 1$ which are, in fact, equal to zero. Probably, the reason of this deviation is that the theoretical analysis of the spatial correlation was made with consideration for only main terms of asymptotic expansion of the coherence function for a spherical wave reflected from a mirror.² This approach is justified only when the condition $\beta_0 > 1$ is rigorously fulfilled, which is not realized in our experiment, and we failed to find any theoretical analysis corresponding to the experimental condition for a finite value of β_0 .

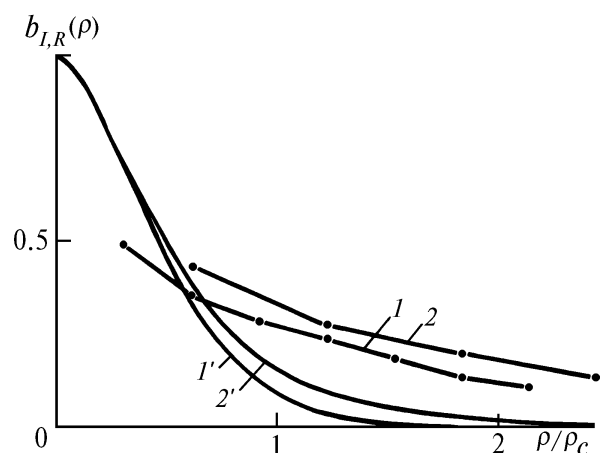


FIG. 3 The spatial correlation coefficient $b_{I,R}(\rho)$ for strong intensity fluctuations of a spherical wave reflected from a plane mirror (1 and 2 are the experimental data and 1' and 2' are the theoretical calculations).

Figure 4 shows the experimental estimates of the temporal cross correlation functions (curves 1 and 2) for different ratios σ_{\perp}/V_{\perp} and receiver separations $\rho = 0.8\sqrt{2\lambda L}$. The value of dimensionless time delay $\tau_{\text{ef}} = \sqrt{\sigma_{\perp}^2 + V_{\perp}^2} \tau / \sqrt{2\lambda L}$, where τ is the time delay, is plotted on the abscissa.

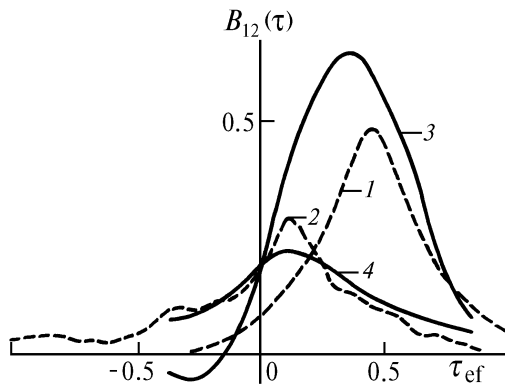


FIG. 4. The cross correlation functions $B_{12}(\tau)$ of the intensity fluctuations for a spherical wave reflected from a plane mirror as a function of the dimensionless time delay τ_{ef} : 1 and 2) experimental data; 3 and 4) theoretical calculations.⁹ $\sigma_{\perp}/V_{\perp} = 0.2(1), 0.25(3), 2.2(2), \text{ and } 4(4)$.

As one can see from the figure, the increase of σ_{\perp}/V_{\perp} from 0.2 (curve 1) to 2.2 (curve 2) leads to lower correlation and shift of the maximum toward shorter time delays. For qualitative comparison, the temporal cross correlation function theoretically calculated in the first approximation of the smooth perturbation method for close separation $\rho_{\text{ef}} = 0.7\sqrt{2\lambda L}$ and $\sigma_{\perp}/V_{\perp} = 0.25$ (curve 3) and 4 (curve 4) (see Ref. 9) are shown in Fig. 4. Different positions of the maxima in theoretical and experimental curves are explained by different separations of the receivers.

As follows from the analysis, all curves of the temporal cross correlation functions for strong fluctuations

of the intensity lie between the limiting dependences corresponding to $\sigma_{\perp} = 0$ and $V_{\perp} = 0$ when the scale of similarity τ_{ef} is used.

Thus the performed experimental studies have shown the existence of the low-frequency shift in the spectra of strong fluctuations of the intensity for a spherical wave reflected from a plane mirror in the turbulent atmosphere when the point of observation is removed in the receiver plane from the strictly backward direction. This shift depends on the ratio of the fluctuational and average components of wind velocity in the direction perpendicular to the propagation path. The results that have been obtained show the inhomogeneity in the spatial correlation for strong fluctuations of the intensity in the image plane. This qualitatively confirms the results of theoretical calculations.^{1,2} It is shown that the temporal cross correlation functions for strong fluctuations of the spherical wave intensity behave analogously to the correlation function of the wave propagated on a straight path⁹ when the scale of similarity τ_{ef} is used.

REFERENCES

1. V.E. Zuev, V.A. Banakh, and V.V. Pokasov, *Optics of the Turbulent Atmosphere* (Gidrometeoizdat, Leningrad, 1988), 270 pp.
2. V.A. Banakh and V.L. Mironov, *Lidar Propagation of Laser Radiation in the Turbulent Atmosphere* (Nauka, Novosibirsk, 1986), 173 pp.
3. A.S. Gurvich, A.P. Ivanov, S.S. Kashkarov, et al., *Atmos. Oceanic Opt.* **5**, No. 1, 29 (1992).
4. A.P. Ivanov, G.Ya. Patrushev, and A.P. Rostov, *Atm. Opt.* **2**, No. 9, 774 (1989).
5. A.P. Rostov, *Opt. Atm.* **1**, No. 3, 125 (1988).
6. J.S. Bendat and A.G. Piersol, *Random Data: Analysis and Measurement Procedures* (Wiley, New York, 1971).
7. E.A. Monastyrnyi, G.Ya. Patrushev, and V.V. Pokasov, *Opt. Spektrosk.* **56**, No. 1, 41 (1984).
8. M.V. Anisimov, E.A. Monastyrnyi, G.Ya. Patrushev, and A.P. Rostov, *Prib. Tekh. Eksp.*, No. 4, 196 (1988).
9. E.A. Monastyrnyi and G.Ya. Patrushev, *Radiotekh. Elektron.* **33**, No. 10, 2183 (1988).